Factor analysis of inelastic electron scattering cross section spectra of $FeSi_2$

IOP Conf. Series: Materials Science and Engineering **467** (2019) 012010 doi:10.1088/1757-899X/467/1/012010

Factor analysis of inelastic electron scattering cross section spectra of $FeSi_2$

A. Yu. Igumenov[1], A. S. Parshin[1], V. O. Kanzychakova[1], A. M. Demin[2], T. A. Andryushchenko[1], Yu. L. Mikhlin[3], O. P. Pchelyakov[4], V. S. Zhigalov[5]

[1]Reshetnev Siberian State University of Science and Technology, 660037, Krasnoyarsk, Russia.
[2]Emperor Alexander I St. Petersburg State Transport University, 190031, Saint Petersburg, Russia.
[3]Institute of Chemistry and Chemical Technologies of the Siberian Branch of the Russian Academy of Sciences, 660036, Krasnoyarsk, Russia.
[4]Rzhanov Institute of Semiconductor Physics of the Siberian Branch of the Russian Academy of Sciences, 630090, Novosibirsk, Russia.
[5]Kirensky Institute of Physics of the Siberian Branch of the Russian Academy of Sciences, 660036, Krasnoyarsk, Russia.

E-mail: aparshin2010@mail.ru

Abstract. Iron disilicide is widely used in creation of such nanotechnology devices as photoelectric converters. The investigation of iron silicide $FeSi_2$ with the method of inelastic electron scattering cross-section spectroscopy was carried out. The decomposition of inelastic electron scattering cross-section spectra of $FeSi_2$ to bulk and surface energy loss components using factor analysis was carried out. The amplitude of energy loss components can be used for identification of their origin.

1. Introduction

An iron disilicide system is promising for basic research and practical applications in devices of nanoelectronics, spintronics and photonics [1]. Elemental analysis of Fe-Si structures is complicated by the formation of the silicides because the chemical shifts in X-ray photoelectron spectra (XPS) practically do not depend on the iron silicide composition [1, 2] and bulk plasmon energy in reflection electron energy loss spectra (REELS) obtained by different authors give conflicting results [3].

In this paper the results of iron disilicide investigation using inelastic electron scattering cross-section spectroscopy was carried out. The decomposition of inelastic electron scattering cross-section spectra of $FeSi_2$ to bulk and surface energy loss components using factor analysis was carried out. The amplitude of energy loss components can be used for identification of their origin.

2. Experimental part

Iron silicide $FeSi_2$ was produced by melting a mixture of iron and silicon in atomic ratio of 1×2 under high vacuum conditions using the vacuum deposition installation UVN-2M-1. The mixture was maintained at the melting temperature for 15 min, after which the annealed alloy was crushed and again melted for 15 min. The 1 mm thick washers were cut of bulk samples. Before the spectroscopic investigations the washers were polished.

The spectroscopic experiments were carried out using a photoelectron spectrometer SPECS (German production) equipped with the spherical energy analyzer PHOIBOS MCD9, double anode X-ray tube as an X-ray source, and a Microfocus EK-12-M electron gun (STAIB Instruments) for excitation of the REEL spectra. The surface contaminations, protecting layers and oxide layers were removed applying Ar^+ ion etching (accelerating voltage of 2.5 kV, ion current of 15 μA) with an ion source IQE-12/38 (SPECS) in the analytical chamber of the spectrometer before the REELS measurements; the completeness of the procedure was controlled via the relevant photoelectron and Auger spectra.

REEL spectra were acquired in the interval of 150 eV below the elastic peak with an energy step of 0.1 eV. Energy loss T was calculated as the difference between the primary electron beam energy E_0 (zero loss) and the reflected electron energy E, $T = E_0 - E$. The primary electron beam energies were 300, 600, 1200, 1900, 3000 eV, and the full width at half-maximum (FWHM) of the primary electron beam was less than 1 eV.

The inelastic electron scattering cross section spectra (so-called $K\lambda$-spectra [4]) which are the products of inelastic mean free path λ and inelastic scattering cross-section K (E_0, T) were calculated from the experimental reflection electron energy loss spectra with the software package QUASES^{TM} XS REELS (Quantitative Analysis of Surfaces by Electron Spectroscopy cross section determined by REELS) [5] based to the algorithm suggested in [6]. Inelastic electron scattering cross section spectra indicate the probability of electron energy loss T in a single scattering event. $K\lambda$-spectra can be used for quantitative determination of element concentrations in two-component composite structures. The ability of quantitative determination of atomic element concentrations in Fe_xSi_{1-x} [7, 8], Mn_xSi_{1-x} [7] and Ge_xSi_{1-x} [10] systems were investigated earlier with the dependence of the maximum value of $K\lambda$-spectra for the standard samples.

The results of applying FA for investigation of inelastic electron scattering cross section spectra of Si, SiO_2, GaAs are presented in [11,12]. The procedure of FA contains two main steps. The first step (principal component analysis (PCA)) yields a minimum number N of principal components (abstract factors). These components are necessary to adequately describe the data. This procedure reduces the data matrix dimensionality into the lowest dimensionalities which are sufficient to adequately describe the data. The second step (target transformation (TT)) transforms the main N abstract factors into physically meaningful factors.

In the PCA step, the Kλ-spectra are placed into a data matrix. The m measured with different E0 Kλ-spectra, having p energy data points were arranged in columns to form a data matrix D(p×m). From this, the covariance matrix $D\cdot D^{T}=(p\times p)$ was constructed by multiplying the data matrix D by its transpose. The eigenfunctions were determined by finding a matrix U, which satisfies $[D\cdot D^{T}]\cdot[U]=[x]\cdot[U]$. This is an eigenvalue problem of the covariance matrix $D\cdot D^{T}$ to obtain the diagonal matrix of eigenvalues $[x]$ and the matrix of eigenvectors [U]. The resulting eigenvectors were arranged in order of magnitude of the corresponding eigenvalues. The data matrix D can be expressed as a linear expansion of these principal components which are also called abstract factors. Only the abstract factors which correspond to the large eigenvalues are needed to get a good account of the data, whereas, those with smaller eigenvalues can be neglected. Although the abstract factors give a perfect mathematical model of the data matrix D, they have no physical meaning.

In the second step, we obtain physically meaningful factors by TT of the principal abstract factors. Transformation can be performed by means of target rotation. This rotation corresponds to multiply abstract factors with a transformation matrix to give new factors. In the "present" case, we have two major factors. This means the factor space has two dimensions, and a two-dimensional transformation matrix, involving an orthogonal rotation angle θ,

$$T = \begin{pmatrix} \cos(\theta) & \sin(\theta) \\ -\sin(\theta) & \cos(\theta) \end{pmatrix}$$

is first applied for a TT.

It is well known that bulk-loss component can be described by a formula of Tougaard. In Ref. [13-19] the method of inelastic electron scattering cross-section spectra fine structure analysis was suggested. The fine structure analysis is based on fitting $K\lambda$-spectra to the 3 parameters Lorentzian-type formula of Tougaard [20]:

$$\lambda K = \frac{BT}{\left(C - T^2\right)^2 + DT^2}.$$

B, C, D are fitting parameters and have special values for different elements [20]. The peak intensity depends on parameter *B*, peak energy depends on parameter *C*, peak width and, indirectly, peak energy depend on parameter *D*.

With this orthogonal rotation, we obtain the first dominant real component corresponding to the bulk-loss component. We applied these criteria for the bulk-loss component determination and changed the factor axes rotation angle until the first factor fitted well to a formula of Tougaard.

If the second component corresponding to the surface-excitation component given by this orthogonal rotation is not adequate from the physical viewpoint, an additional oblique rotation (with rotation angle φ) of one axis is done to get the second real component. After the coordinate rotation of two primitive abstract factors, the real factors with physical meaningful features are thus obtained.

3. Results and discussion

3.1. $FeSi_2$ inelastic electron scattering cross-section spectra

Fig. 1 (a) shows the inelastic electron scattering cross-section spectra for $FeSi_2$ silicide. The main peak energy increases monotonically with increasing of primary electron energy in inelastic electron scattering cross-section

spectra (Fig. 1 (b)). With increasing of primary electron energy increases the depth analysis, resulting in decreasing of surface-like excitation intensity and increasing of bulk-like excitation intensity.

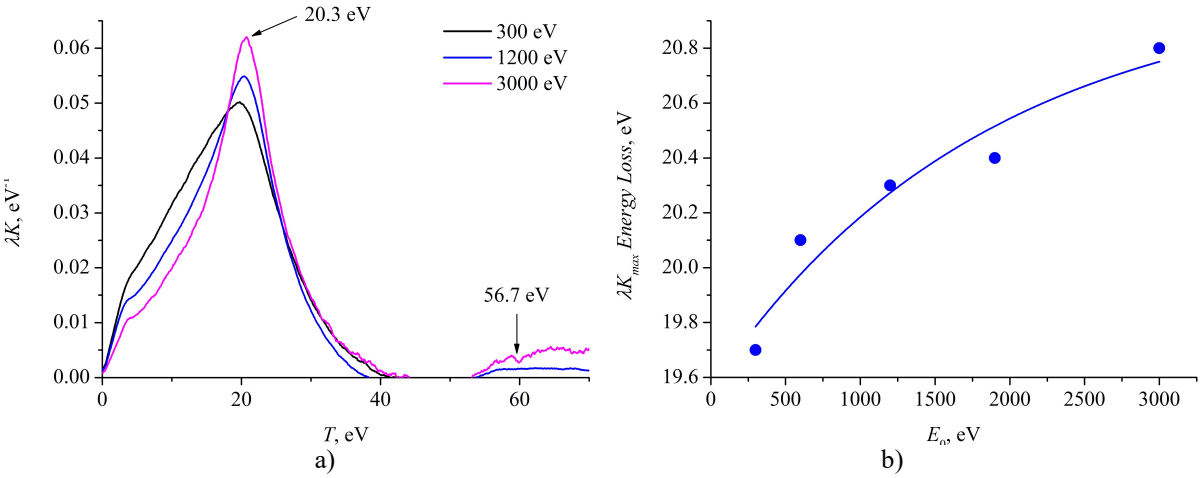

Figure 1. Inelastic electron scattering cross-section spectra (a) and the primary energy dependence of main peak loss energy (b)

This intensity redistribution causes a change of the whole spectrum shape and peak position. The presence of unresolved surface plasmon in $K\lambda$-spectra of iron silicides manifests itself in decreasing of FWHM. Further, to isolate the surface and bulk contributions, the FA will be applied.

3.2. Factor analysis of $FeSi_2$ inelastic electron scattering cross-section spectra

Fig. 2 (a) shows the reconstruction of $K\lambda$-spectra of $FeSi_2$ for E_0 = 300 eV (a) and E_0 = 3000 eV (b) by a linear combination of surface electronic excitation and bulk-loss components

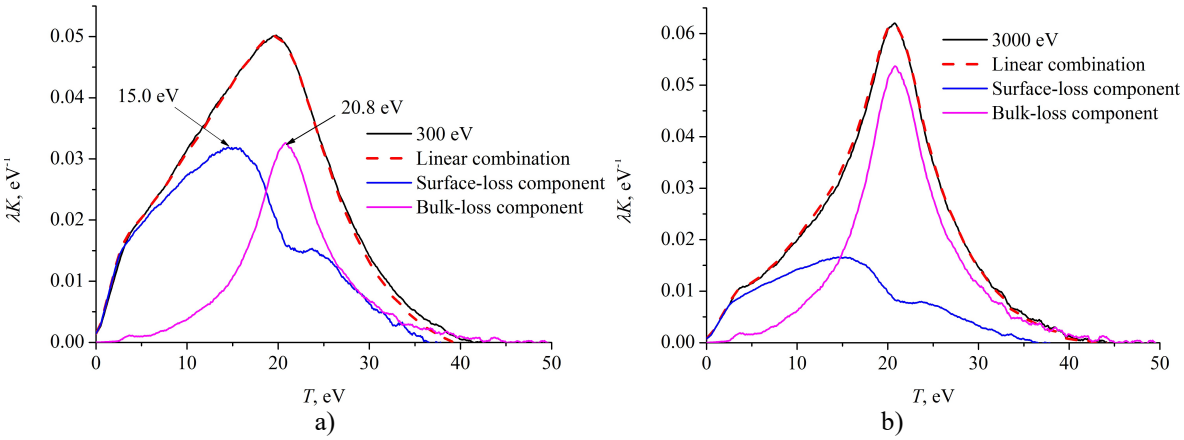

Figure 2. Reconstruction of $K\lambda$-spectra of $FeSi_2$ for E_0 = 300 eV (a) and E_0 = 3000 eV (b) by a linear combination of surface electronic excitation and bulk-loss components

Obtaining real factors for $FeSi_2$, we selected the angle in a way that the bulk-loss component should be well-approximated to the Tougaard peak, similarly done for the surface one, but it turned out much worse. This is because the surface contribution is unresolved. The obtained values of the energies of the bulk and surface components are close to the literature values for the energy of the bulk and surface plasmons [3].

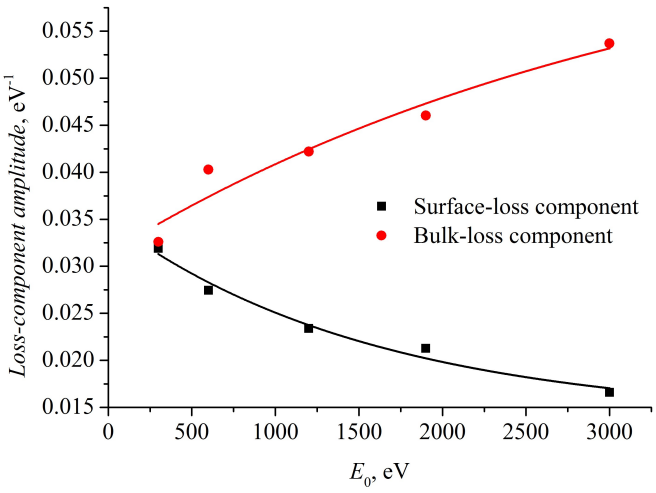

Figure 3. The primary energy dependences of the loss-component amplitude

The bulk-loss component has gradually increasing primary energy dependence of amplitude which indicate its volume origin (Fig. 3). The surface-loss component has gradually decreasing primary energy dependence of amplitude. The surface-loss component was unresolved in $K\lambda$-spectra for $FeSi_2$ but FA allows determining its energy, intensity and origin.

4. Conclusions

The inelastic electron scattering cross-section spectra for silicide $FeSi_2$ were investigated. It was shown that these spectra contains unresolved surface energy losses. Decomposition of $FeSi_2$ to surface and bulk energy loss components using factor analysis allowed to identify the unresolved energy losses, determine their energies, intensities and origin. It is shown that the amplitude of energy-loss components can be used for identification of their origin.

References

[1] Ohtsu N., Oku M., Satoh K., Wagatsuma K., 2013 *Appl. Surf. Sci.* **264** pp 219-224.
[2] Ohtsu N., Oku M., Nomura A., Sugawara T., Shishido T., Wagatsuma K. 2008 *Appl. Surf. Sci.* **254** pp 3288-3294.
[3] Lifshits V. G., Lunyakov Yu. V. 2004 Electron Energy Loss Spectra of Surface Phases on Silicon *Vladivostok: Dal'nauka*.
[4] Gergely G. *2002 Prog. Surf. Sci.* **71** pp 31-88.
[5] Tougaard S. QUASES – Software packages to characterize surface nano-structures by analysis of electron spectra http, available at: http://www.quases.com/.
[6] Tougaard S., Chorkendorff I. 1987 *Phys Rev. B* **35** pp 6570-6577.
[7] Parshin A. S., Pchelyakov O. P., Dolbak A. E., Ol'shanetskii B. Z., 2013 *Journal of Surface Investigation. X-ray, Synchrotron and Neutron Techniques* **7** pp 505-508.
[8] Parshin A. S., Aleksandrova G. A., Dolbak A. E., Pchelyakov O. P., Ol'shanetskii B. Z. , Ovchinnikov S. G. , Kushchenkov S. A. 2008 *Tech. Phys. Letters* **34** pp 381-383.
[9] Parshin A. S., Kushchenkov S. A., Aleksandrova G. A., Ovchinnikov S. G. 2011 *Tech. Phys.* **56** pp 656-661.
[10] Parshin A. S., P'yanovskaya E. P., Pchelyakov O. P., Mikhlin Yu. L. , Nikiforov A. I., Timofeev V. A. , Esin M. Yu. 2014 *Semiconductors* **48** pp 224-227.
[11] Jin H., Shinotsuka H., Yoshikawa H., Iwai H., Tanuma S., Tougaard S. *Journal of applied physics* 2010 **107** pp 083709.
[12] Jin H., Shinotsuka H., Yoshikawa H., Iwai H., Arai M., Tanuma S., Tougaard S. *Surface and Interface Analysis* 2013 **45** pp 985–992.
[13] Parshin A.S., Igumenov A.Yu., Mikhlin Yu.L., Pchelyakov O.P., Zhigalov V.S., 2016 *Physics of the Solid State* **58** pp 908-914.
[14] Parshin A.S., Igumenov A.Yu., Mikhlin Yu.L., Pchelyakov O.P., Nikiforov A.I., Timofeev V.A., 2015 *Semiconductors* **49**, **4** pp 423-427.

[15] Parshin A.S., Igumenov A.Yu., Mikhlin Yu.L., Pchelyakov O.P., Nikiforov A.I., Timofeev V.A., 2014 *Vestn. Sib. Gos. Aerokosm. Univ.* **4 (56)** pp 230-235.
[16] Parshin A.S., Igumenov A.Yu., Mikhlin Yu.L., Pchelyakov O.P., Zhigalov V.S., 2016 *IOP Conference Series: Materials Science and Engineering* **122** pp 012025, 1-7.
[17] Parshin A.S., Igumenov A.Yu., Mikhlin Yu.L., Pchelyakov O.P., Zhigalov V.S., 2016 *Technical Physic* **61 (9)** pp 1418-1422.
[18] Parshin A.S., Igumenov A.Yu., Mikhlin Yu.L., Pchelyakov O.P., Zhigalov V.S., 2016 *Izvestiya Vysshikh Uchebnykh Zavedenii, Fizika* **59, 10** pp 82-86.
[19] Parshin A.S., Igumenov A.Yu., Mikhlin Yu.L., Pchelyakov O.P., Zhigalov V.S., 2016 *IOP Conference Series: Materials Science and Engineering* **255** pp 012019, 1-7.
[20] Tougaard S. 1997 *Surf. Interface Anal.* **25** pp 137-155.